

Technologies and Materials for Renewable Energy, Environment & Sustainability

Gas Sensing Study Using Tin Oxide Thin Film for Hydrogen Sulfide Gas

AIPCP25-CF-TMREES2025-00026 | Article

PDF auto-generated using **ReView**



Gas Sensing Study Using Tin Oxide Thin Film for Hydrogen Sulfide Gas

Zinah Abdulateef Abbas^{1, a)} and Seham Hassan Salman^{2, b)}

¹*Al-Nahrain Research Center for Renewable Energy, AL-Nahrain University, Jadriya, Baghdad 10072, Iraq.*

²*Department of Physics, College of Education for Pure Science / Ibn Al-Haitham, University of Baghdad, Baghdad, Iraq.*

^{a)} Corresponding author: zinah.a.a@nahrainuniv.edu.iq

^{b)} seham.h.s@ihcoedu.uobaghdad.edu.iq

ABSTRACT: Tin (Sn) films with a thickness of (400±20) nm were prepared by the thermal evaporation method, and the samples were then oxidized at 300 and 400 °C. X-ray diffraction was used to study the crystal structure and phase of the film before and after oxidation. The surface morphology was examined by AFM, and the optical properties were analyzed by spectroscopy in the wavelength range of 300-1100 nm. It was observed that the maximum transmittance was less than 70%, and the energy gap increased with increasing oxidation temperature. The film oxidized at 400 °C was tested for H₂S gas sensing when the film was exposed to different temperatures and a fixed concentration (20ppm). It was found that the sensitivity increased with increasing temperature, with the highest sensitivity being 0.806, the response time being 22.5 seconds, and the recovery time being 49.5 seconds at 200 °C.

Keywords: SnO; films: sensing properties; H₂S gas.

INTRODUCTION

Known transparent semiconductor oxides exhibit both n-type and p-type conductivity. P-type transparent semiconductor oxides are few in number and perform less well than their n-type counterparts. In most p-type oxide semiconductors, the valence band arises from highly oriented oxygen p orbitals, which severely restrict carrier transport in a slightly disordered structure [1]. However, in SnO, contributions from Sn 5s states near the top of the valence band significantly facilitate gap mobility and are therefore considered a suitable candidate for the development of oxide-based active electronic devices [2]. Tin oxide (SnO) is a p-type material with an optical energy gap of approximately 2.7–2.9 eV and carrier mobility of approximately 7 cm²/V/s, so it is used in many applications including gas sensing, p-n diodes, transistors, and solar cells [3–4]. Given the effects of H₂S gas on humans, it must be detected and special sensors developed. This highly toxic gas has a foul odor similar to that of rotten eggs. It is produced by combustion processes, vehicle emissions, volcanic eruptions, and other processes. Submerged areas and salt mines are also major sources of H₂S gas [5,6]. SnOx films can be fabricated using various techniques, and both pure and doped films are used to sense gases such as nitrogen dioxide [7], carbon monoxide [8–9], ethanol [10], methane [11], hydrogen sulfide [5], ammonia [12–13]. In this paper, the possibility of obtaining tin oxide thin film phases using thermal evaporation and simple oxidation methods was investigated, and the physical properties of the deposited samples were examined. Finally, we fabricated a hydrogen sulfide gas sensor at a constant concentration and different operating temperatures.

EXPREMENTAL

Sn thin films were prepared by thermal evaporation technique. Sn metal were kept in the Mo boat. The vacuum chamber was evacuated with a two stage rotary pump followed by diffusion pump to a base vacuum of 3×10^{-6} Torr. Tin metal was evaporated on glass substrates (2*2 cm) supplied by Carborundum Universal Ltd., Hosur, India) by resistive heating of Mo boat. Substrates were kept at a temperature of 400 °C during the deposition process. The deposition rate was kept in the range of 10^{-15} Å s⁻¹. Final thickness of the thin films was 400nm. These thin film samples were oxidation at temperatures in the range of (300 – 400) °C under oxygen flowing for 1 hours. Tin thin films were deposited by thermal evaporation technique. Tin metal was evaporated onto German-made glass substrates (2 × 2 cm), in a vacuum of (2×10^{-5}) mbar by resistively heating a molybdenum boat with a voltage of 60 V. The substrates were kept at a temperature of 450 °C during the deposition process. The deposition time was approximately

11 minutes and the final thickness of the thin films reached 400 ± 20 nm, as determined by the molecular weight and optical method. The second step was to oxidize the samples in an oven at temperatures of (300-400) °C in the presence of oxygen for an hour and then leave the samples to cool. Crystal structure are studied by (XRD) and AFM. Optical characteristics are studied within range 300-1100 nm and band gap are calculated. To fabricate the gas sensor, aluminum electrodes were deposited by thermal evaporation in a comb pattern on the sample surface with various dimensions

RESULTS AND DISCUSSION

Structural Characterization

Figure (1) shows the X-ray diffraction (XRD) patterns of the as-deposited (Sn) thin films and the thin films after oxidation at a temperature of (300- 400) °C. Figure (1) shows that the diffraction pattern of the films oxidized at 300 °C contains four peaks for the (SnO_2) phase, three peaks for the (Sn_3O_4) phase, and two peaks for the (SnO) phase.

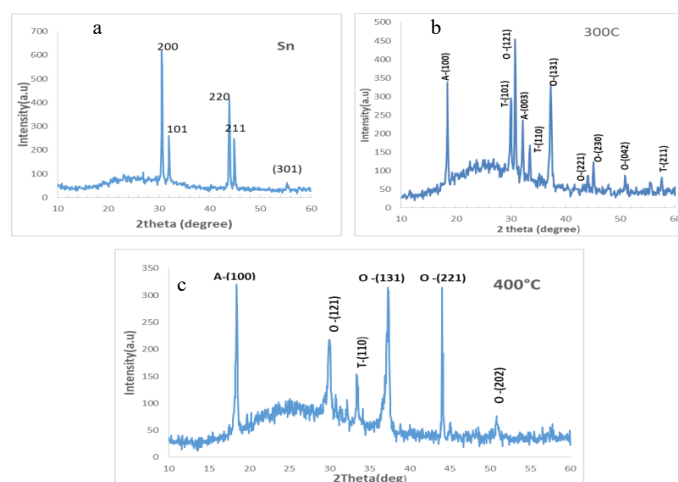


FIGURE 1a,b,c. XRD pattern of (Sn) and SnOx thin films

TABLE 1. Information obtained from XRD examination.

Temp. exidation (°C)	Card No.	phase	2Θ _{abs.}	2Θ A stand.	d _{abs} (deg)	d _{A stand}	hkl	
Sn	00-002-0709	Sn-T	30.647	30.644	2.9147	2.915	200	
			43.902	43.871	2.0606	2.062	220	
			44.928	44.902	2.0159	2.017	211	
300	98-018-1280	SnO ₂ -O	30.847	30.909	2.8962	2.891	121	
		SnO ₂ -O	37.31	37.16	2.408	2.417	131	
		00-020-1293	Sn ₃ O ₄ -A	18.527	18.315	4.785	4.840	100
400	98-018-1280	SnO ₂ -O	37.284	37.160	2.4097	2.417	131	
		00-020-1293	Sn ₃ O ₄ -A	18.494	18.315	4.793	4.79	100
		98-018-1280	SnO ₂ -O	44.059	44.314	2.053	2.042	221

The diffraction pattern of the films oxidized at 400 °C contains four peaks for the (SnO₂) phase and one peak for the (SnO and Sn₃O₄) phase. This indicates increased crystallinity and dominance of the (SnO₂) phase. This is consistent with the optical properties, as the energy gap became (3.1eV) due to the (SnO₂) phase. The JCPDS card numbers and (hkl) values are shown in Table 1. The crystallite size of thin films is calculated from equation (1). [14-17]

$$C_s = \frac{0.94\lambda}{\beta \cos\theta} \quad (1)$$

The dislocation density δ , microstrain ε and N_o were calculated through the following relationships: [18-23]

$$\delta = \frac{1}{C_s^2} \quad (2)$$

$$\varepsilon = \frac{\beta \cos\theta}{4} \quad (3)$$

$$N_o = \frac{t}{C_s^3} \quad (4)$$

It is also observed from table 2 the crystal size decreases 32.9 to 24.6nm with increase oxidation temp. from 300 °C to 400 °C.

TABLE 2. hkl, 2 θ , phase, C_s , δ , ε and N_o

Temp. (°C)	Hkl	2 θ_{abs}	phase	$\beta_{FWHMdeg}$	C.s nm	δ (line/m ² *10 ⁻³	ε *10 ⁻³	N_o
300	121	30.847	SnO ₂	0.2623	32.818	0.9284	1.102	0.0113
400	131	37.285	SnO ₂	0.3564	24.691	1.6402	1.465	0.0265

Surface Morphology

The AFM images showed that the surface of the SnO thin film was topographically formed from hills and valleys that are distributed uniformly over the entire film surface.

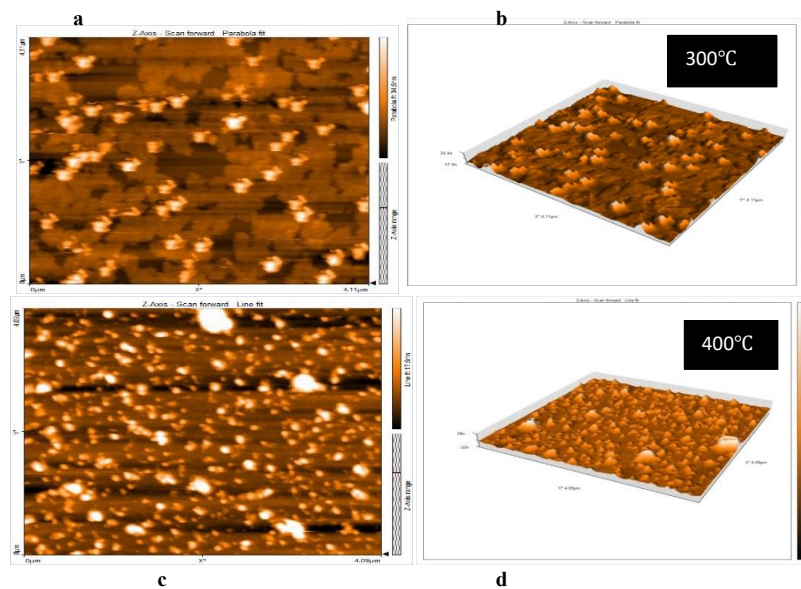


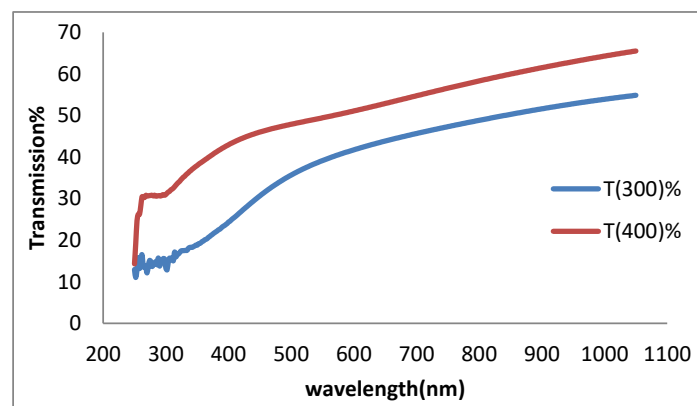
FIGURE 2. The AFM image for SnOx films

TABLE 3. AFM parameters

Oxidation temp.(°C)	Mean diameter(nm)	Roughness(nm)	Root-mean-square (nm)
300	59.74	3.178	5.865
400	30.78	6.313	8.836

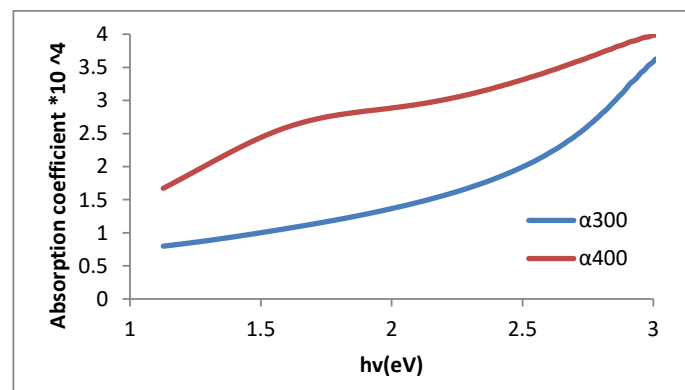
The Optical Properties

The transmission of tin oxide thin films are shown in Fig. 3 change the wavelength in the region of 300 nm – 1100 nm. The average transmission of the SnO₂ films was less than 70% over 400nm.

FIGURE 3. Transmission of the SnO₂ thin films.

From the relationship number (5) the absorption coefficient was calculated. [15].

$$\alpha = \frac{2.303A}{t} \quad (5)$$

FIGURE 4. Absorption coefficient (α) vs ($h\nu$)

The band gap energy (E_g) is determined using the equation [15, 24]:

$$\alpha(h\nu) = A (h\nu - E_g)^r \quad (6)$$

Figure 5 represents a plot of $(\alpha h\nu)^2$ versus photon energy for the thin films. The band gap energy was found to be 2.8 eV for the oxide sample at 300 °C and 3.1 eV for the oxide sample at 400 °C, with the band gap increasing due to structural defects and oxygen vacancies.

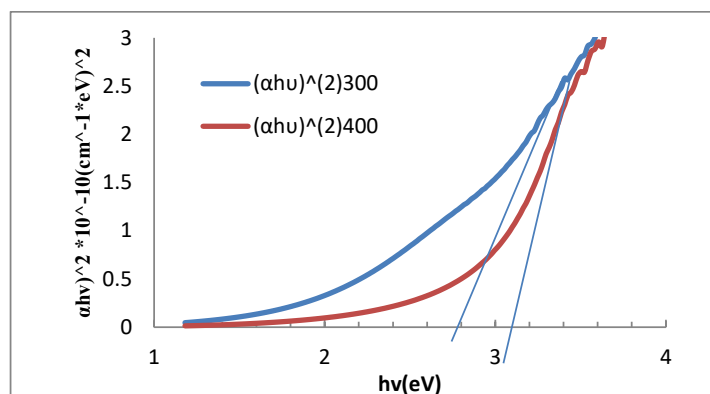


FIGURE 5. Energy gap of SnO₂ thin film at different oxidation temp.

TABLE 4. Shows Absorption coefficient and Eg

Temp. Oxidation (°C)	$\alpha(\text{cm}^{-1}) \cdot 10^4$	Eg (eV)
300	3.437228	2.8
400	2.45451	3.1

The Sensitivity Results

$$S = \frac{R_g - R_a}{R_a} \times 100\% \quad (7)$$

The equation (7) [14] was used to calculate gas sensitivity, where R_a represents the background resistance of the membrane in the absence of the gas, and R_g represents the final resistance of the membrane in the presence of the gas. Figure 6 shows the change in resistance over time for a sample oxidized at 400°C. It was found that as the temperature applied during the membrane's exposure to the gas increased, the gas sensitivity increased [25-27].

Also, nickel oxide films prepared by the thermal evaporation method show a response to hydrogen sulfide gas at a concentration of 20ppm at an oxidation temperature of 700°C [28].

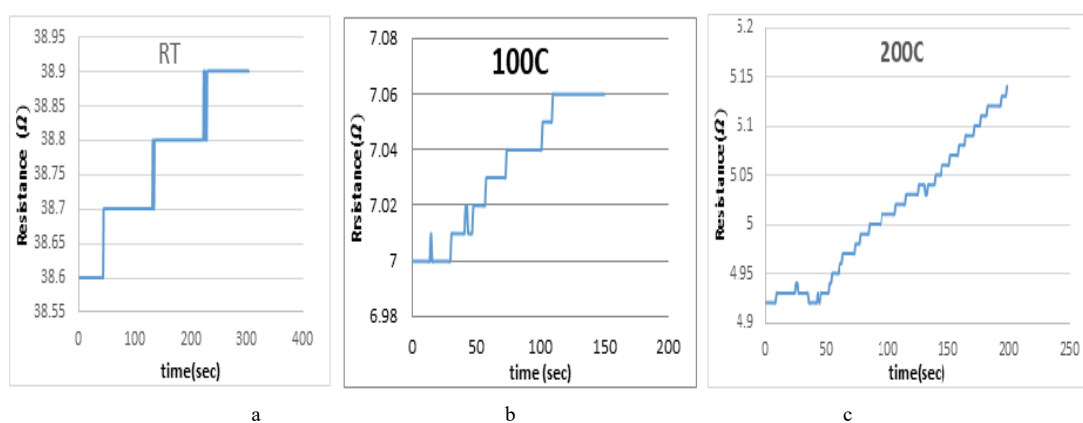


FIGURE 6 a, b, c. The resistance changes with the time of SnO₂ films.

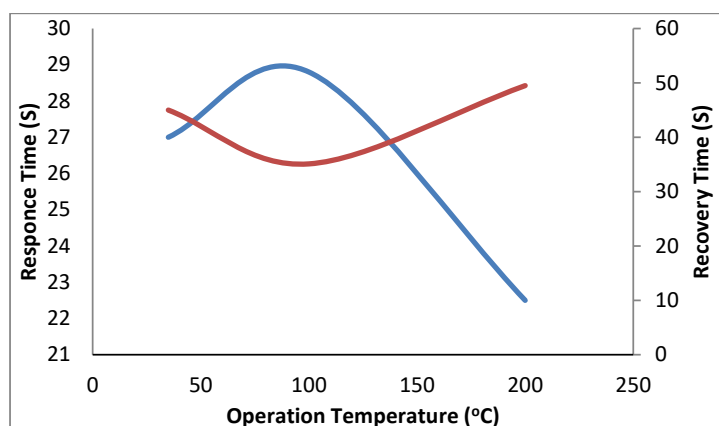


FIGURE 7. The response and recovery times drop exponentially with operation temperature.

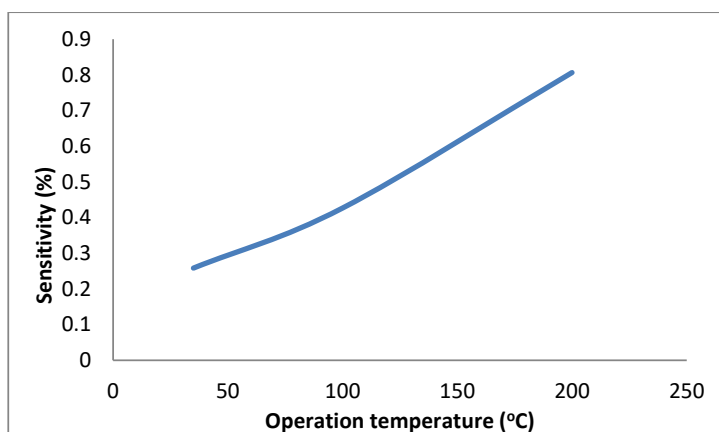


FIGURE 8. Sensitivity changes with operation temp.

TABLE 5. S%, response and recovery time for thin films at (R.T,100,200) °C for gas (H₂S).

Operating Temp. (°C)	Sensitivity (S%)	response time (sec)	Recover time (sec)
35	0.2583	27	45
100	0.4267	28.8	35.1
200	0.8064	22.5	49.5

Table 5 shows that sensitivity improves with increasing operating temperature, with the highest sensitivity and lowest response time at 200°C (0.806 for 20 ppm gas). The response and recovery times were 22.5 seconds and 49.5 seconds, respectively.

CONCLUSION

SnO_x films were prepared by thermal evaporation technique. X-ray diffraction (XRD) and atomic force microscopy (AFM) studies revealed crystallite size (32.8-24.68) nm and Mean diameter (59.7-30.7) nm. The band gap was (2.6-3.2) eV through optical measurement of the films oxidized at 300 and 400 °C. SnO₂ thin-film sensors demonstrated the highest sensitivity and lowest response time at 200°C to H₂S gas.

REFERENCES

1. J.S. Kachirayil, Y.P. Venkata Subbaiah, K. Tian and A. Tiwari, "P-type SnO thin films and SnO/ZnO heterostructures for all-oxide electronic and optoelectronic device applications," *Thin Solid Films* 605, 193–200 (2016). <https://doi.org/10.1016/j.tsf.2015.09.026>
2. Q.-J. Liu, Z.-T. Liu and L.-P. Feng, "First-principles calculations of structural, electronic and optical properties of tetragonal SnO₂ and SnO," *Comput. Mater. Sci.* 47, 1016–1022 (2010). <https://doi.org/10.1016/j.commatsci.2009.11.038>
3. Z. Wang, P.K. Nayak, J.A. Caraveo-Frescas and H.N. Alshareef, *Adv. Mater.* 28, 3831 (2016). <https://doi.org/10.1002/adma.201503080>
4. W. Guo, L. Fu, Y. Zhang, K. Zhang, L.Y. Liang, Z.M. Liu, H.T. Cao and X.Q. Pan, "Microstructure, optical, and electrical properties of p-type SnO thin films," *Appl. Phys. Lett.* 96, 042113 (2010). <https://doi.org/10.1063/1.3277153>
5. R. Kumar, "Hydrogen sulfide gas sensing properties of SnO₂ thin films prepared by thermal evaporation technique," *J. Phys.: Conf. Ser.* 1531, 012013 (2020). <https://doi.org/10.1088/1742-6596/1531/1/012013>
6. B. Elvers, S. Hawkins and G. Schulz (eds.), *Ullmann's Encyclopedia of Industrial Chemistry*, Vol. A15 (VCH, Weinheim, 1990), p.55.
7. H.J. Abdul-Ameer, M.F. AL-Hilli and M.K. Khalaf, "Comparative NO₂ sensing characteristics of SnO₂:WO₃ thin film against bulk and investigation of optical properties," *Baghdad Sci. J.* 15, 227–233 (2018). <http://dx.doi.org/10.21123/bsj.2018.15.2.0227>
8. S.K. Tripathy and T.N.V.P. Rao, "Thermally evaporated tin oxide thin film for gas sensing applications," *J. Nano-Electron. Phys.* 9, 02019 (2017). [https://doi.org/10.21272/jnep.9\(2\).02019](https://doi.org/10.21272/jnep.9(2).02019)
9. I.D.P. Hermida, G. Wiranto, Hiskia and R. Nopriyanti, "Fabrication of SnO₂ based CO gas sensor device using thick film technology," *J. Phys.: Conf. Ser.* 776, 012061 (2016). <https://doi.org/10.1088/1742-6596/776/1/012061>
10. Vishwakarma, A. K., Mishra, A. K., & Srivastava, S. "Sensing performance of lead monoxide-doped tin oxide thick film gas sensor", *Bulletin of Materials Science*, Vo.47(3) ,(2024). <https://doi.org/10.1007/s12034-024-03270-9>
11. Ahmed, B.A., Mohammed, J.S., Fadhil, R.N., ...Shaban, A.H., Al Dulaimi, A.H., The dependence of the energy density states on the substitution of chemical elements in the Se6 Te4-xSbx thin film, *Chalcogenide Letters*, 2022, 19(4), pp. 301–308.
12. B.A. Hasan, "SnO₂ doped In₂O₃ thin films as reducing gas sensors," *IOP Conf. Ser.: Mater. Sci. Eng.* 928, 072011 (2020). <https://doi.org/10.1088/1757-899X/928/7/072011>
13. Bagga, S., Akhtar, J., & Mishra, S. (2020). Ammonia gas sensing with tin oxide thin film sensor and coplanar microheater. *AIP Conference Proceedings*, 2294, 020004. <https://doi.org/10.1063/5.0031525>
14. S.H. Salman, N.A. Hassan and G.S. Ahmed, "Copper telluride thin films for gas sensing applications," *Chalcogenide Lett.* 19, 125–130 (2022). <https://doi.org/10.15251/cl.2022.192.125>
15. K. Al Abdullah, F. Al Alloush, M. J. Termanini, and C. Salame, "Low frequency and low temperature behavior of Si solar cell by AC impedance measurements," *Energy Procedia* 19, 183–191 (2012).
16. D. Hadi, H. Hadi and S.H. Salman, "Effect of annealing on the physical characteristics of In₂O₃ nanoparticle films," *Ann. Chim. Sci. Matér.* 49, 315–320 (2025). <https://doi.org/10.18280/acsm.490311>
17. A.H.A. Alrazak, S.H. Salman, I.A. Abbas, M.H. Mustafa, H.M. Ali and S.A. Abbas, "Influence of doping with silver nanoparticles on the molybdenum trioxide gas sensor prepared by spray pyrolysis," *Digest J. Nanometer. Biostructures* 20, 191–199 (2025). <https://doi.org/10.15251/djnb.2025.201.191>
18. S. H. Salman, S. M. Ali, and G. S. Ahmed, "Study the Effect of Annealing on Structural and Optical Properties of Indium Selenide (InSe) Thin Films Prepared by Vacuum Thermal Evaporation Technique," *J. Phys.: Conf. Ser.* 1879, 032058 (2021). <https://doi.org/10.1088/1742-6596/1879/3/032058>
19. S.H. Salman, S.S. Jahil, N.A. Hassan, S.A. Abbas and K.A. Jasim, "Ammonia gas sensing using porous silicon," *J. Phys.: Conf. Ser.* 2857, 012051 (2024). <https://doi.org/10.1088/1742-6596/2857/1/012051>
20. Al Hilli, B., Abood, Z. A., and Mehdi, M. S. "The effect of substrate nature on the properties of tin sulfide Nanostructured films prepared by chemical bath deposition". *Ibn AL-Haitham Journal for Pure and Applied Sciences*, 36(3), 85-90. (2023). <https://doi.org/10.30526/36.3.3020>
21. Shatha F. Abbas, Hiba M. Ali," Improving the properties of NiO films by doping with copper nanoparticles', *Journal of Physics: Conference Series* 3028 (2025) 012044, <https://doi.org/10.1088/1742-6596/3028/1/012044>
22. N.A. Hassan and I.H. Khudayer, "Thickness effect of CuAlTe₂ thin films on morphological, structural and visual properties," *Ibn Al-Haitham J. Pure Appl. Sci.* 33, 3 (2020). <https://doi.org/10.30526/33.3.2471>
23. S. H. Salman, A. A. Shihab, and A. H. K. Eltayef, "Studying the Effect of the Type of Substrate on the Structural, Morphology and Optical Properties of TiO₂ Thin Films Prepared by RF Magnetron Sputtering," *Energy Procedia* 157, 199–207 (2019). <https://doi.org/10.1016/j.egypro.2018.11.181>
24. N.A. Hassan, Z.N. Jaf, S.H. Salman, I.H. Khudayer, H. Ibrahim and H.A. Miran, "Influence of In-dopant on the optoelectronic properties of thermal evaporated CuAlTe₂ films," *Solid State Commun.* 371, 115260 (2023). <https://doi.org/10.1016/j.ssc.2023.115260>
25. I.A. Abbas and S.Q. Hazaa, S.H. Salman, "Employment of titanium dioxide thin film on NO₂ gas sensing," *J. Phys.: Conf. Ser.* 1879, 032061 (2021). <https://doi.org/10.1088/1742-6596/1879/3/032061>

26. M.H. Faisal and S.H. Salman, "Effect of oxidation times on gas sensitivity and characterization for In_2O_3 thin films produced by thermal evaporation," *J. Phys.: Conf. Ser.* 2857, 012010 (2024). <https://doi.org/10.1088/1742-6596/2857/1/012010>
27. S.H. Salman, A.A. Shihab and A.-H.Kh. Elttayef, "Design and construction of nanostructure TiO_2 thin film gas sensor prepared by RF magnetron sputtering technique," *Energy Procedia* 157, 283–289 (2019). <https://doi.org/10.1016/j.egypro.2018.11.192>
28. Dastan, D., Shan, K., Jafari, A., Marszalek, T., Mohammed, M. K., Tao, L., Shi, Z., Chen, Y., Yin, X., Alharbi, N. D., Gity, F., Asgary, S., Hatamvand, M., and Ansari, L. Influence of heat treatment on H_2S gas sensing features of NIO thin films deposited via thermal evaporation technique. *Materials Science in Semiconductor Processing*, (2023) 154, 107232. <https://doi.org/10.1016/j.mssp.2022.107232>